The EMBO Journal Vol.17 No.5 pp.1192–1199, 1998

The structure of the tetratricopeptide repeats of protein phosphatase 5: implications for TPR-mediated protein–protein interactions

Amit K.Das, PatriciaT.W.Cohen[1] and David Barford[2]

Laboratory of Molecular Biophysics, University of Oxford, Rex Richards Building, South Parks Road, Oxford, OX1 3QU and [1]MRC Protein Phosphorylation Unit, Department of Biochemistry, University of Dundee, Dundee, DD1 4HN, UK

[2]Corresponding author
e-mail: davidb@biop.ox.ac.uk

The tetratricopeptide repeat (TPR) is a degenerate 34 amino acid sequence identified in a wide variety of proteins, present in tandem arrays of 3–16 motifs, which form scaffolds to mediate protein–protein interactions and often the assembly of multiprotein complexes. TPR-containing proteins include the anaphase promoting complex (APC) subunits cdc16, cdc23 and cdc27, the NADPH oxidase subunit p67 phox, hsp90-binding immunophilins, transcription factors, the PKR protein kinase inhibitor, and peroxisomal and mitochondrial import proteins. Here, we report the crystal structure of the TPR domain of a protein phosphatase, PP5. Each of the three TPR motifs of this domain consist of a pair of antiparallel α-helices of equivalent length. Adjacent TPR motifs are packed together in a parallel arrangement such that a tandem TPR motif structure is composed of a regular series of antiparallel α-helices. The uniform angular and spatial arrangement of neighbouring α-helices defines a helical structure and creates an amphipathic groove. Multiple-TPR motif proteins would fold into a right-handed super-helical structure with a continuous helical groove suitable for the recognition of target proteins, hence defining a novel mechanism for protein recognition. The spatial arrangement of α-helices in the PP5–TPR domain is similar to those within 14-3-3 proteins.

Keywords: Protein crystallography/protein phosphatase/protein phosphorylation/signal transduction/tetratricopeptide repeat

Introduction

Reversible protein phosphorylation on serine and threonine residues is essential for the regulation of numerous cellular functions and signal transduction pathways. Control of this process is achieved by the modulation of the activities and substrate specificities of the protein kinases and phosphatases, which catalyse the opposing phosphorylation and dephosphorylation reactions, respectively. The protein Ser/Thr phosphatase PP5 is the prototype of the fourth subfamily of the PPP-family of protein phosphatases, which also includes PP1, PP2A and PP2B (calcineurin) (Barford, 1996; Cohen, 1997). PP5 is conserved from yeast to humans being predominantly, although not exclusively, nuclear in location (Chen *et al.*, 1994). In mammals, PP5 has a widespread tissue distribution. Elevated levels of PP5 in rapidly growing cells compared with serum-deprived cells suggest a role in cell growth (Cohen *et al.*, 1996).

The primary structure of PP5 reveals a C-terminal catalytic domain and an N-terminal tetratricopeptide repeat (TPR) domain containing three tandem TPR motifs (Becker *et al.*, 1994; Chen *et al.*, 1994; Chinkers, 1994) (Figure 1). TPRs occur in over 25 proteins of diverse biological functions and are known to mediate protein–protein interactions (Goebl and Yanagida, 1991; Sikorski *et al.*, 1991; Lamb *et al.*, 1995) (Figure 1). Within PP5, the TPR domain may perform several roles. Firstly, the TPR domain is responsible for the >25-fold stimulation of protein phosphatase activity by polyunsaturated fatty acids such as arachidonic acid (Chen and Cohen, 1997; Skinner *et al.*, 1997). The interaction of arachidonic acid with the TPR domain induces an allosteric conformational change within PP5 that abolishes the suppression of catalytic activity by the TPR domain (Chen and Cohen, 1997). The activity of the arachidonic acid-stimulated PP5 is similar to that of the isolated PP5 phosphatase domain that has been proteolytically cleaved from the TPR domain. A second role of the TPR domain of PP5 is to mediate interactions between PP5 and hsp90 within an hsp90–glucocorticoid receptor complex, and also with the kinase domain of the ANP-guanylate cyclase receptor *in vivo*, findings which are consistent with a role for PP5 in signal transduction (Chinkers, 1994; Silverstein *et al.*, 1997). However, it is not known whether interactions between the TPR domain of PP5 and hsp90 stimulate the PP5 phosphatase activity. In addition to its interactions with PP5, hsp90 also associates with the TPR-containing immunophilins FKBP52 and Cyp40, in a mutually exclusive manner (Owens-Grillo *et al.*, 1996; Ratajckak and Carrello, 1996).

The TPR motif was first identified as a tandemly repeated degenerate 34 amino acid sequence in the cell division cycle genes *cdc16*, *cdc23* and *cdc27* which encode subunits of the anaphase promoting complex (APC) (Hirano *et al.*, 1990; Sikorski *et al.*, 1990; King *et al.*, 1995). The role of the APC is to target cell cycle proteins for ubiquitin-dependent degradation at both the onset of anaphase and at the exit of mitosis. Mutations within the TPR motifs of these proteins cause mitotic arrest at the metaphase to anaphase transition. It is now realised that over 25 proteins present in organisms as diverse as bacteria and humans contain TPR motifs. In addition to cell cycle regulation, processes such as transcription control, mitochondrial and peroxisomal protein transport, neurogenesis, protein kinase inhibition, Rac-mediated activation of NADPH oxidase, and protein folding involve TPR motifs (Lamb *et al.*, 1995; Ponting,

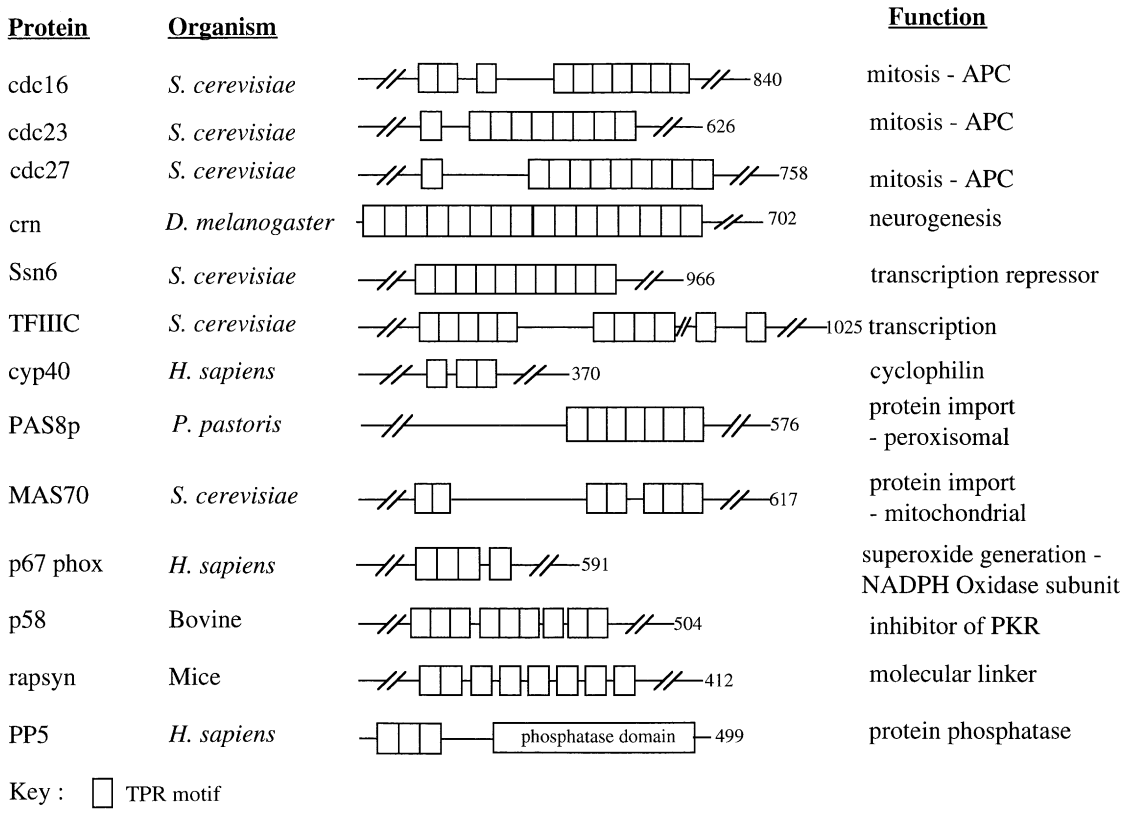

Fig. 1. Schematic of TPR-containing proteins. TPR motifs (shown as boxes) are observed as multiple tandem repeats and also separated by sequence insertions.

1996). Moreover, a 10 tandem TPR motif protein (UTY) was recently identified as one of the 12 novel genes of the non-recombining region of the human Y-chromosome (Lahn and Page, 1997).

Within TPR-containing proteins, the TPRs are usually arranged in tandem arrays of 3–16 motifs, although individual, or blocks, of TPR motifs may be dispersed throughout the protein sequence (Figure 1). Mutagenesis and deletion studies have revealed roles for TPR motifs in mediating protein–protein interactions. Proteins with multiple copies of TPR motifs function as scaffolding proteins and coordinate the assembly of proteins into multi-subunit complexes. Such proteins include Ssn6, cdc16, cdc23, cdc27 and rapsyn (Ponting and Phillips, 1996). Rapsyn for example, has been proposed to act as a molecular link between the nicotinic acetylcholine receptor and the dystrophin–dystroglycan complex (Apel *et al.*, 1995). Specific blocks of TPR motifs mediate interactions with particular target proteins and have been assigned specific biological functions. For example, the N-terminal three TPR motifs of Ssn6 associate with the co-repressor Tup1, whereas other combinations of TPR motifs mediate interactions with different transcription factors, which accounts for the diverse gene expression patterns regulated by Ssn6 (Smith *et al.*, 1995; Tzamarias and Struhl, 1995). TPR motifs 5–7 of p58, an inhibitor of the RNA-dependent protein kinase (PKR), are responsible for interactions with PKR, while the N-terminal TPR motifs direct homotypic interactions (Gale *et al.*, 1996). TPR motifs 1–3 of the peroxisomal import protein PAS8p interact with the peroxisomal targeting signal (Terlecky *et al.*, 1995). Within the multi-subunit APC, a mutation in TPR7 of cdc27 reduced its ability to interact with cdc23 but did not affect its interactions with itself or with cdc16 (Lamb *et al.*, 1994).

In order to understand the molecular basis for TPR-mediated protein recognition, we have determined the crystal structure of the TPR domain of PP5 to 2.5 Å resolution. The results provide insight into the structure of multiple TPR motif proteins, the basis for disruptive mutations within the TPR-containing subunits of the APC and NADPH oxidase and reveal a novel mechanism for protein–protein interactions.

Results and discussion

Structure determination and overall structure

The crystal structure of the N-terminal TPR domain of PP5 was determined to 2.5 Å resolution using multiple isomorphous replacement and anomalous scattering methods. Electron density maps obtained using experimental phases were readily interpretable (Figure 2) and the polypeptide chain was traced within continuous density.

The three tandem TPR motifs of PP5 reveal a novel protein fold. Each TPR motif is composed of a pair of antiparallel α-helices, termed helices A and B, associated together with a packing angle of ~24° between helix axes (Figure 3A–C). The structure of each TPR motif is virtually identical; main-chain atoms of TPR1 superimpose with those of TPR2 and TPR3 with a root mean square deviation (r.m.s.d.) of 0.35 Å and 0.8 Å, respectively. The three TPR motifs are organised into a parallel arrangement, such that sequentially adjacent α-helices are antiparallel in a manner reminiscent of a concertina (Figure 3A–C).

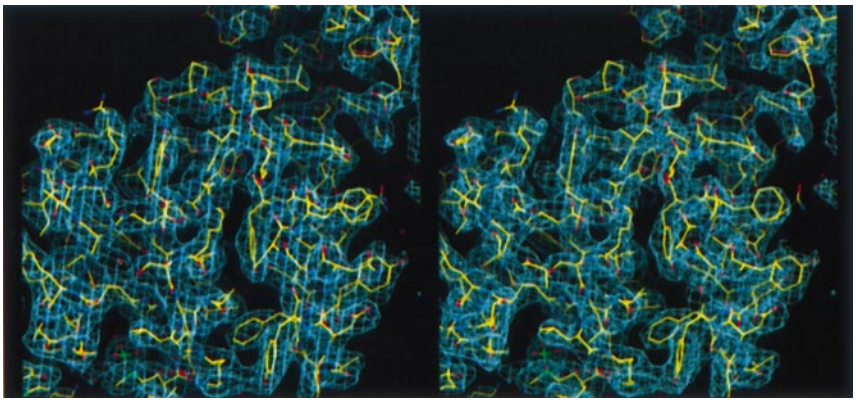

Fig. 2. Stereo view of the electron density map of the PP5–TPR domain calculated to 2.5 Å resolution using experimental phases with the refined coordinates superimposed. The figure was produced using O (Jones *et al.*, 1991).

Within a tandem array of TPR motifs, the packing of helix A against adjacent B-helices is defined by the same spatial and angular parameters both within, and between, adjacent TPR motifs. Hence, in general, each α-helix shares two immediate α-helix neighbours and the protein fold may be defined as an overlapping array of three-helix bundles.

Multiple sequence alignments of the TPRs present in >25 proteins reveals a highly degenerate sequence. Although there is no position characterised by an invariant residue, a consensus sequence pattern of small and large hydrophobic residues has been defined (Figure 3D). Small hydrophobic residues are commonly observed at positions 8, 20 and 27 within the motif. Position 32 is frequently a proline and large hydrophobic residues are also located at particular positions. Analysis of the structure of the TPR domain of PP5 provides a rationale for this consensus sequence pattern (Figure 3C and D). Residues 8 and 20 are located at the position of closest contact between the A and B α-helices of a TPR, whereas residue 27 on helix B is located at the interface of 3 helices (A, B and A′) within a 3-helix bundle. Proline 32 is located at the C-terminus of helix B, and the large consensus hydrophobic residues form the interfaces between adjacent α-helices. Mutations at position 8 of TPR3 of the NADPH oxidase subunit p67 phox and within TPRs 5 and 7 of the APC subunit cdc23 result in the disruption of protein function, presumably due to the incorrect packing of neighbouring α-helices (Figure 3D) (Sikorski *et al.*, 1993; de Boer *et al.*, 1994). The Gly to Glu substitution in p67 phox is associated with chronic granulomatous disease and impairment of NADPH oxidase activity (de Boer *et al.*, 1994). The TPR region of p67 phox is the site of NADPH oxidase recognised by the small G-protein Rac, hence disruption of TPR3 may prevent Rac-stimulation of the enzyme activity (Diekmann *et al.*, 1994; Ponting, 1996). In yeast, individual mutations at position 8 of TPR5 and TPR7 of cdc23 (Sikorski *et al.*, 1993) and position 20 of TPR9 of Cut9 (Samejima and Yanagida, 1994) (a cdc16 homologue) result in mitotic arrest at the metaphase to anaphase transition, most likely as a result of a blockade in the ubiquitin-dependent degradation of inhibitors of this transition.

The 35-residues C-terminal to the three TPR motifs of PP5, while sharing weak sequence similarity to a TPR motif, are folded into an extended α-helix (α7). This helix packs against helix B of TPR3 in a similar arrangement to that of the helices within the TPR domain (Figure 3A–C). The consequence of a regular repeat of α-helices that are related by a crossover angle of 24° is to generate a right-handed helical conformation that creates an amphipathic channel (Figure 4). The surface of the channel is formed predominantly by the side chains of amino acids in helix A of each TPR motif with relatively little contribution from residues of helix B. In contrast, the opposite side of the channel is formed by residues from both TPR α-helices.

Structural relationship to 14-3-3 proteins

The antiparallel arrangement of α-helices of the TPR domain of PP5 is reminiscent of the antiparallel α-helices of the 14-3-3 protein, a homodimeric molecule with nine α-helices in each subunit (Liu *et al.*, 1995; Xiao *et al.*, 1995) (Figure 5). Unlike TPR proteins however, the α-helices of 14-3-3 proteins vary in length and in their relative packing geometries and only three of the seven α-helices of the TPR domain superimpose closely (r.m.s.d. of 1.2 Å) with equivalent α-helices of 14-3-3 (Figure 5). TPR-containing proteins and 14-3-3 proteins share common structural and functional properties, despite their lack of sequence similarities (Aitken, 1996). The latter proteins interact with proteins phosphorylated on Ser/Thr residues, most probably via an amphipathic groove present within each 14-3-3 subunit that is similar to the groove observed in the PP5–TPR domain. Within the PP5–TPR domain crystals, the protein forms a homodimer as a result of the antiparallel association of symmetry-related α-7 helices and the interaction of residues C-terminal to α-7 with residues forming the channel surface of the same symmetry-related molecule (Figure 4). Similar to the crystal structure of the τ-isoform of 14-3-3 (Xiao *et al.*, 1995), a sulfate ion is bound within this groove by a cluster of basic residues, and this sulfate ion interacts with the channel-bound peptide. The interaction of a peptide within the groove of the TPR domain, as observed in the PP5–TPR domain crystals, may provide a model for the recognition of phosphopeptides by 14-3-3 proteins. However, the TPR-mediated dimer does not occur in full-length PP5

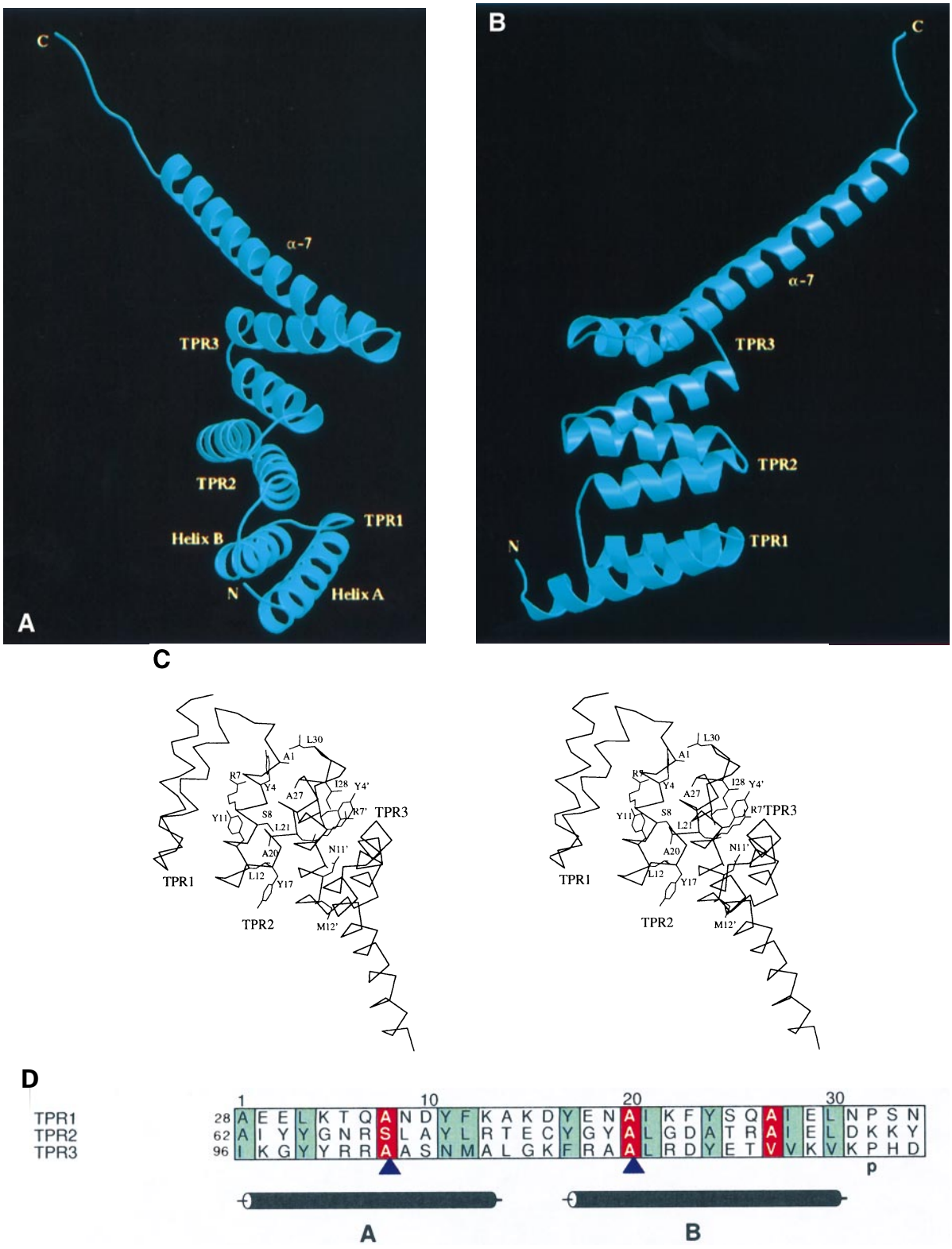

Fig. 3. (**A** and **B**) Two orthogonal views of ribbon representations of the TPR domain of PP5. Each TPR motif and the α-7 helix are labelled. The sequence of α-7 shows weak similarity to a TPR motif. Helix A of TPR1 is extended by nine residues N-terminal to the TPR domain. (**C**) Stereo view of the molecule. Within TPR2 and helix A of TPR3, consensus TPR motif residues (Figure 3D) are drawn to illustrate their role in inter-helix packing. The residue numbering refers to the TPR motif numbering. Primes denote residue numbering in TPR3. Main-chain atoms of any pair of helices superimpose onto equivalent atoms of all other pairs of helices within an r.m.s.d. of 1.1 Å. Figures drawn using MOLSCRIPT (Kraulis, 1991). (**D**) Sequence alignment of the three TPR motifs of PP5. Consensus TPR motif residues are shown with red and green backgrounds for small and large hydrophobic residues, respectively. The position of the consensus proline residue is indicated with a P. The sites of mutations in the NADPH oxidase subunit p67 phox (position 8; de Boer *et al.*, 1994), cdc23 (position 8; Sikorski *et al.*, 1993) and cdc16 (position 20; Samejima and Yanagida, 1994) are indicated with blue arrows. Numbers above the alignment refer to TPR motif residues and at the side, to the PP5 residues. The figure was prepared using ALSCRIPT (Barton, 1993).

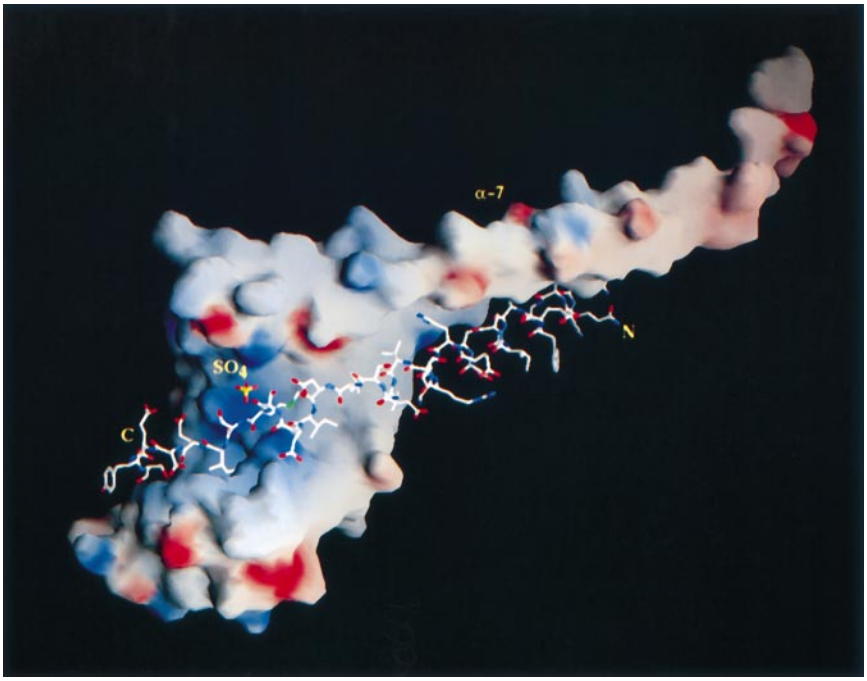

Fig. 4. Solvent accessible surface of the PP5–TPR domain showing the electrostatic potential and amphipathic TPR-groove. Atoms of the α-7 helix of the symmetry-related molecule are shown interacting with the α-7 helix and the C-terminus with the amphipathic groove. The sulfate ion is labelled. The figure was drawn using GRASP (Nicholls and Honig, 1991).

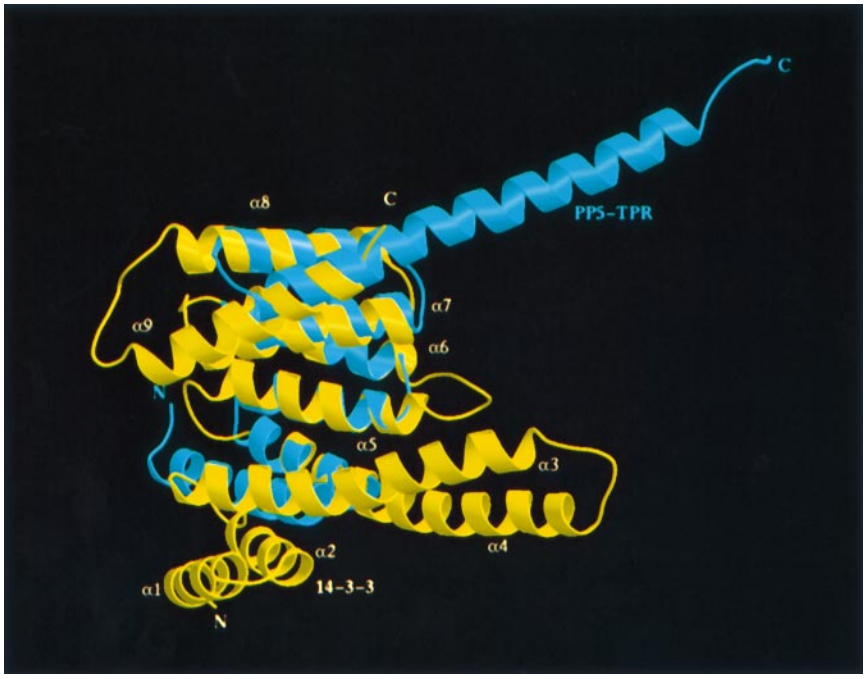

Fig. 5. Comparison of the structures of the TPR domain of PP5 (cyan) and a 14-3-3 protein (Liu *et al.*, 1995) (yellow). Helices 4–6 of 14-3-3 were superimposed onto equivalent main-chain atoms of helices B, A and B of TPR motifs 1 and 2 with a r.m.s.d. of 1.2 Å. The figure was drawn using MOLSCRIPT (Kraulis, 1991).

which is a monomer, as judged by size exclusion chromatography.

Protein recognition by multiple TPR motif proteins

Our model of the three TPR motifs of PP5 provides a framework for predicting the structures of other TPR-motif-containing proteins and for interpreting functional studies of these proteins. To understand the properties of multiple-motif TPR proteins, we constructed a model of 12 tandem TPR motifs. We assumed that the packing parameters between adjacent TPR motifs of the tandem repeat would be similar to those observed in the TPR domain of PP5. The resultant model indicates that tandemly arranged TPR motifs are organised into a regular right-handed super-helix with a helical repeat of approximately seven TPR motifs, a pitch of 60 Å and a

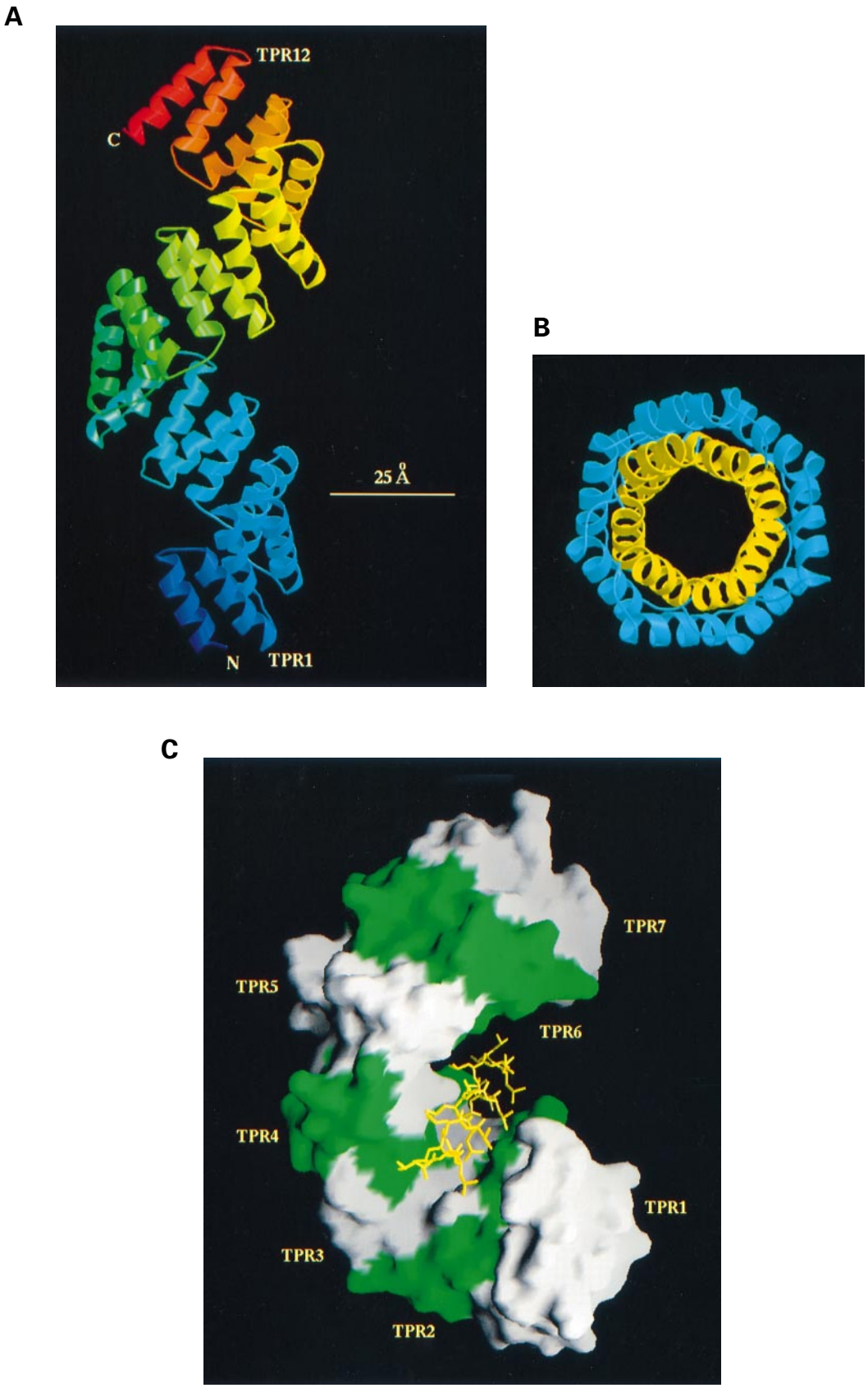

Fig. 6. Model of a multiple TPR motif containing protein. (**A**) View perpendicular to the helix axis of 12 TPR motifs. The main-chain is colour ramped from blue at the N-terminus to red at the C-terminus. (**B**) View parallel to the helix axis of an 8-motif TPR protein. A and B helices are coloured yellow and cyan, respectively. (**C**) Surface representation of a 7-motif TPR helix indicating that a poly-leucine α-helix may be accommodated within the extended helical groove of the protein. The surface of alternate TPR motifs are coloured white and green. The figures were drawn using MOLSCRIPT (Kraulis, 1991) and GRASP (Nicholls and Honig, 1991).

Table I. Data collection, phase determination and refinement statistics

	Native	Derivatives	
		EMTS[a]	TMLA[b]
Space group	I422	I422	I422
Cell parameters a (Å)	90.06	90.06	90.94
c (Å)	104.45	104.45	105.52
Z (N)	16	16	16
X-ray source	PX96[c]	PX96	PX95[d]
Resolution (Å)	2.45	2.45	2.45
Unique reflections (N)	7832	7959	5033
Completeness (%)	96.8	97.5	66
Redundancy	2.9	4.36	2.5
R_{sym} (I)[e] (%)	7.3	7.2	8.0
Phasing power (centric/acentric)[f]	–	1.26/1.70	0.64/0.56
Number of sites	–	3	1
Figure of merit of MIRAS from 24–2.5Å: 0.42 (0.83 after solvent flattening)			
Refinement			
Resolution range (Å)	15–2.45		
Reflections used (R_{free} set)	6751 (1045)		
R_{cryst}/R_{free}	0.201/0.298		
Protein (solvent) atoms (N)	1281 (78)		
Sulfate ions (N)	2		
R.m.s.d. bond lengths (Å)/angles (°)	0.012/1.754		

[a]EMTS, ethyl mercurithiosalicylate 1.0 mM incubation for 3 h.
[b]TMLA, trimethyl lead acetate, 20 mM incubation for 3 days.
[c]PX96: Station PX9.6, SRS, Daresbury, UK.
[d]PX95: Station PX9.5, SRS, Daresbury, UK.
[e]R_{sym} $\Sigma_h\Sigma_i |I_{(h)}-I_{i(h)}| / \Sigma_h\Sigma_i I_{i(h)}$ where $I_{i(h)}$ and $I_{(h)}$ are the ith and the mean measurements of the intensity of reflection h.
[f]Root mean square ($<F_H>/E$) where F_H is the heavy atom structure factor amplitude and E is the residual lack of closure error.
R_{cryst} $\Sigma\{|F_o|-|F_c|\} / \Sigma|F_o|$ where $|F_o|$ and $|F_c|$ are the observed and calculated structure factor amplitudes respectively. R_{free} is calculated for a randomly chosen reflection omitted from the refinement, and R_{cryst} is calculated for the remaining reflections included in refinement.

width of 42 Å (Figure 6A). The inside face of the TPR helix is formed by α-helix A of each TPR motif with the B α-helix located on the outside of the TPR helix (Figure 6B). The groove observed in the three-TPR motif structure of PP5 (Figures 3 and 4) is extended to form a continuous groove on the inside of the TPR helix, and is ideally suited to accept an α-helix of a target protein (Figure 6C). Five to six TPR motifs could contribute to the interactions with a bound α-helix. Amino acid insertions between TPRs may be readily accommodated on the outer face of the super-helix, which could also allow the assembly of protein complexes or, as has been proposed for cdc27, perform other biological functions such as DNA recognition (Hirano *et al.*, 1990). The TPR helix formed by TPR-containing proteins would allow such proteins to interact simultaneously with multiple target proteins, utilising specific combinations of TPR motifs within the super-helix, consistent with mutagenesis and deletion studies and with the assembly function of a scaffolding protein (Smith *et al.*, 1995; Terlecky *et al.*, 1995; Tzamarias and Struhl, 1995; Gale *et al.*, 1996). The role played by TPR proteins to coordinate multi-subunit assembly is similar to that played by the cytoskeletal protein β-catenin, which is composed of 12 copies of a 42 residue armadillo repeat. β-catenin binds to numerous proteins including cadherins, the tumor suppressor gene product Adenomatous Polyposis Coli and Tcf-family transcription factors. Significantly, the crystal structure of the armadillo repeats of β-catenin shares structural similarities with TPR proteins as it consists of a right-handed super-helix of α-helices possessing a long positively charged groove predicted to be the site of multi-protein–protein interactions (Huber *et al.*, 1997).

In conclusion, the structure of the TPR domain of PP5 provides a basis for understanding protein–protein interactions mediated by TPR-motif-containing proteins, revealing a novel mechanism for molecular recognition. The model of TPR-mediated protein recognition that we present here will serve as a basis for the design of experiments to elucidate the roles of individual TPR motifs and of specific amino acid residues in this mechanism. Future studies will be aimed at revealing the basis for the recognition of hsp90 and polyunsaturated fatty acids by the TPR domain of PP5 and the mechanism of regulation of protein phosphatase activity.

Materials and methods

Protein purification and crystallization

The cDNA encoding the N-terminal domain (Arg 16 to Leu 181) of human PP5, preceded and terminated by the vector sequences MARIRA and LGMM, respectively, was expressed from the pT7.7 vector in *Escherichia coli* at 20°C (Chen and Cohen, 1997). The TPR domain is within residues 28–129 and the phosphatase catalytic domain of PP5 starts at approximately residue 186 (Chen *et al.*, 1994). Protein purification to homogeneity was performed using five purification steps: (i) *S*-Sepharose cation exchange chromatography; (ii) Mono-Q anion exchange chromatography; (iii) phenyl-TSK hydrophobic interaction chromatography; (iv) gel filtration using a Pharmacia Superose S75 column and (v) Mono-S cation exchange chromatography. The purified protein was dialysed into 10 mM Tris–HCl pH 7.5, 50 mM NaCl, 2 mM dithiothreitol (DTT) and concentrated to 9 mg/ml (assuming an extinction coefficient at 280 nm of 1.0 per 1 mg/ml of protein). Crystallizations were performed at 4°C using the vapour diffusion method with a precipitant of 1.8 M ammonium sulfate, 4% (v/v) 2-methyl-2,4-pentanediol (MPD), 100 mM HEPES pH 7.5 and 2 mM DTT. Tetragonal crystals appeared within 7 days and grew to the dimensions 0.3×0.2×0.05 mm. All X-crystallographic data were collected at 100 K. Crystals were transferred into a cryoprotection buffer consisting of 2.0 M ammonium sulfate, 4% MPD, 100 mM HEPES pH 7.5, 50 mM NaCl and 17.5% glycerol, before flash freezing in a nitrogen gas stream.

Structure determination

All data were collected using MAR imaging plates at stations PX9.5 and PX9.6, SRS, Daresbury and processed using DENZO and SCALEPACK (Otwinowski and Minor, 1997). The protein phases were obtained from mercury (EMTS)- and lead (TMLA)-derivatives (Table I). Heavy-atom site refinement and phase calculations were performed using SHARP (de La Fortelle and Bricogne, 1997). The phases calculated using SHARP were improved using iterative solvent flattening (solvent content of 0.57) by SOLOMON (Abraham and Leslie, 1996) and the histogram matching algorithm by DM (Cowtan, 1994). The electron density map calculated to 2.5 Å resolution was readily interpreted and model building performed by means of O (Jones *et al.*, 1991), and atomic coordinates were refined using X-PLOR (Brunger, 1992). The refined model has 90.5% of the residues in the most favoured region and 9.5% in the additionally allowed region of the Ramachandran plot. The N-terminal three residues and C-terminal four residues that are not visible in the electron density map are assumed to be disordered. All other residues are clearly visible within the electron density maps. The mercury heavy-atoms sites were located at Cys 139 and two sites corresponding to two positions adopted by the side-chain of Cys 77. The lead site is coordinated by the side chains of Cys 77 and Glu 56 from a symmetry-related molecule.

The structure of the multiple-TPR-containing super-helix was generated by superimposing equivalent main-chain atoms of TPR1 onto TPR3 of PP5 to create a five-TPR-motif model. TPR1 of PP5 was then

superimposed onto TPR5 of the model to produce a seven-TPR-motif model. This process was repeated until 12 TPR motifs were generated.

Acknowledgements

We thank M.Groves for helpful discussions, M.X.Chen for construction of the PP5–TPR domain expression vector, S.J.Gamblin and R.Liddington for the 14-3-3 protein coordinates and staff at stations PX9.5 and PX9.6, SRS, Daresbury for access to synchrotron facilities. The work was supported by MRC and Wellcome grants to D.B. and MRC funds to P.T.W.C. The TPR-domain coordinates and structure factors have been deposited with the Brookhaven Protein Data Base and have been assigned PDB ID codes 1A17 and R1A17SF, respectively.

References

Abraham,J.P. and Leslie,A.G.W. (1996) Methods used in the structure determination of bovine mitochondrial F1 ATPase. *Acta Crystallogr.*, **D52**, 30–42.

Aitken,A. (1996) 14-3-3 and its possible role in co-ordinating multiple signalling pathways. *Trends Cell Biol.*, **6**, 341–347.

Apel,E.D., Roberds,S.L., Campbell,K.P. and Merlie,J.P. (1995) Rapsyn may function as a link between the acetylcholine receptor and the agrin-binding dystrophin-associated glycoprotein complex. *Neuron*, **15**, 115–126.

Barford,D. (1996) Molecular mechanisms of the protein/serine/threonine phosphatases. *Trends Biochem. Sci.*, **21**, 407–412.

Barton,G.J. (1993) ALSCRIPT: a tool to format multiple sequence alignments. *Protein Eng.*, **6**, 37–40.

Becker,W., Kentrup,H., Klumpp,S., Schultz,J.E. and Joost,H.G. (1994) Molecular cloning of a protein Ser/Thr phosphatase containing a putative regulatory tetratricopeptide repeat domain. *J. Biol. Chem.*, **269**, 22586–22592.

Brunger,A.T. (1992) *X-PLOR: version 3.1*. Yale University Press, New Haven, CT.

Chen,M.X. and Cohen,P.T.W. (1997) Activation of protein phosphatase 5 by limited proteolysis or the binding of polyunsaturated fatty acids to the TPR domain. *FEBS Lett.*, **400**, 136–140.

Chen,M.X., McPartlin,A.E., Brown,L. Chen,Y.H., Barker,H.M. and Cohen,P.T.W. (1994) A novel human protein serine/threonine phosphatase, which possesses four tetratricopeptide repeat motifs and localizes to the nucleus. *EMBO J.*, **13**, 4278–4290.

Chinkers,M. (1994) Targeting of a distinctive protein–serine phosphatase to the protein kinase-like domain of the atrial natriuretic peptide receptor. *Proc. Natl Acad. Sci. USA*, **91**, 11075–11079.

Cohen,P.T.W. (1997) Novel protein phosphatases: variety is the spice of life. *Trends Biochem. Sci.*, **22**, 245–251.

Cohen,P.T.W., Chen,M.X. and Armstrong,C.G. (1996) Novel protein phosphatases that may participate in cell signalling. *Adv. Pharmacol.*, **36**, 67–89.

Cowtan,K. (1994) *Joint CCP4 and ESF-EACBM Newsletter on protein crystallography*, **31**, 34–38.

de Boer,M., Hilarius-Stokman,P.M., Hossle,J.-P., Verhoeven,A.J., Graf,N., Kenney,R.T., Seger,R. and Roos,D. (1994) Autosomal recessive chronic granulomatous disease with absence of the 67-kD cytosolic NADPH oxidase component: Identification of mutation and detection of carriers. *Blood*, **83**, 531–536.

de La Fortelle,E. and Bricogne,G. (1997) Maximum-likelihood heavy-atom parameter refinement for the multiple isomorphous replacement and multiwavelength anomalous diffraction methods. *Methods Enzymol.*, **276**, 472–494.

Diekmann,D., Abo,A., Johnston,C., Segal,A.W. and Hall,A. (1994) Interaction of Rac with p67 phox and regulation of phagocytic NADPH oxidase activity. *Science*, **265**, 531–533.

Gale,M.,Jr, Tan,S.-L., Wambach,M. and Katze,M.G. (1996) Interaction of the interferon-induced PKR protein kinase with inhibitory proteins $P58^{IPK}$ and vaccinia virus K3L is mediated by unique domains: implications for kinase regulation. *Mol. Cell Biol.*, **16**, 4172–4181.

Goebl,M. and Yanagida,M. (1991) The TPR snap helix: a novel protein repeat motif from mitosis to transcription. *Trends Biochem. Sci.*, **16**, 173–177.

Hirano,T., Kinoshita,N., Morikawa,K. and Yanagida,M. (1990) Snap helix with knobs and hole: essential repeats in *S.pombe* nuclear protein nuc2. *Cell*, **60**, 319–328.

Huber,A.H., Nelson,W.J. and Weis,W.I. (1997) Three-dimensional structure of the armadillo repeat region of β-Catenin. *Cell*, **90**, 871–882.

Jones,T.A., Zou,J.Y., Cowan,S.W. and Kjeldgaard,M. (1991) Improved methods for building protein models in electron density maps and the location of errors in these models. *Acta Crystallogr.*, **A47**, 110–119.

King,R.W., Peters,J.M., Tugendreich,S., Rolfe,M., Hieter,P. and Kirschner,M.W. (1995) A 20S complex containing cdc27 and cdc16 catalyses the mitosis-specific conjugation of ubiquitin to cyclin B. *Cell*, **81**, 279–288.

Kraulis,P. (1991) MOLSCRIPT: a program to produce both detailed and schematic plots of protein structures. *J. Appl. Crystallogr.*, **24**, 946–950.

Lahn,B.T. and Page,D.C. (1997) Functional coherence of the human T chromosome. *Science*, **278**, 675–680.

Lamb,J.R., Michaud,W.A., Sikorski,R.S. and Hieter,P.A. (1994) Cdc16p, Cdc23p and Cdc27p form a complex essential for mitosis. *EMBO J.*, **13**, 4321–4328.

Lamb,J.R., Tugendreich,S. and Hieter,P. (1995) Tetratricopeptide repeat interactions: to TPR or not to TPR? *Trends Biochem. Sci.*, **20**, 257–259.

Liu,D., Bienkowska,J., Petosa,C., Collier,R.J., Fu,H. and Liddington,R. (1995) Crystal structure of the zeta isoform of the 14-3-3 protein. *Nature*, **376**, 191–194.

Nicholls,A. and Honig,B. (1991) A rapid finite difference algorithm, utilising successive over-relaxation to solve the Poisson–Boltzmann equation. *J. Comput. Chem.*, **12**, 435–445.

Otwinowski,Z. and Minor,W. (1997) Processing x-ray diffraction data collected in oscillation mode. *Methods Enzymol.*, **276,** 307–326.

Owens-Grillo,J.K., Czar,M.J., Hutchison,K.A., Hoffman,K., Perdew,G.H. and Pratt,W.B. (1996) A model of protein targeting mediated by immunophilins and other proteins that bind to hsp90 via tetratricopeptide repeat domains. *J. Biol. Chem.*, **271**, 13468–13475.

Ponting,C.P. (1996) Novel domains in the NADPH oxidase subunits, sorting nexins, and PtdIns 3-kinases: Binding partners of SH3 domains? *Protein Sci.*, **5**, 2353–2357.

Ponting,C.C.P. and Phillips,C. (1996) Rapsyn's knobs and holes: eight tetratricopeptide repeats. *Biochem. J.*, **314**, 1053–1056.

Ratajczak,T. and Carrello,A. (1996) Cyclophilin 40 (CyP-40), Mapping of its hsp90 binding domain and evidence that FKBP52 competes with CyP-40 for hsp90 binding. *J. Biol. Chem.*, **271**, 2961–2965.

Samejima,I. and Yanagida,M. (1994) Bypassing anaphase by fission yeast cut9 mutation: requirement of cut9+ to initiate anaphase. *J. Cell Biol.*, **127**, 1655–1670.

Sikorski,R.S., Boguski,M.S., Goebl,M. and Hieter,P. (1990) A repeating amino acid motif in CDC23 defines a new family of proteins and a new relationship among genes required for mitosis and RNA synthesis. *Cell*, **26**, 307–317.

Sikorski,R.S., Michaud,W.A., Wootton,J.C., Boguski,M.S., Connelly,C. and Hieter,P. (1991) TPR proteins as essential components of the yeast cell cycle. *Cold Spring Harbor Symposia on Quantitative Biology*, **56**, 663–673.

Sikorski,R.S., Michaud,W.A. and Hieter,P. (1993) $p62^{cdc23}$ of *Saccharomyces cerevisiae*: A nuclear tetratricopeptide repeat protein with two mutable domains. *Mol. Cell. Biol.*, **13**, 1212–1221.

Silverstein,A.M., Galigniana,M.D., Chen,M.-S., Owebs-Grillo,J.K., Chinkers,M. and Pratt,W.B. (1997) Protein phosphatase 5 is a major component of the glucocorticoid receptor hsp90 complexes with properties of an FK506-binding immunophilin. *J. Biol. Chem.*, **272**, 16224–16230.

Skinner,J., Sinclair,C., Romeo,C., Armstrong,D., Charbonneau,H. and Rossie,S. (1997) Purification of a fatty acid-stimulated protein–serine/threonine phosphatase from bovine brain and its identification as a homolog of protein phosphatase 5. *J. Biol. Chem.*, **272**, 22464–22471.

Smith,R.L., Redd,M.J. and Johnson,A.D. (1995) The tetratricopeptide repeats of Ssn6 interact with the homeo domain of alpha-2. *Genes Dev.*, **9**, 2903–2910.

Terlecky,S.R., Nuttley,W.M., McCollum,D., Sock,E. and Subramani,S. (1995) The *Pichia pastoris* peroxisomal protein PAS8p is the receptor for the C-terminal tripeptide peroxisomal targeting signal. *EMBO J.*, **14**, 3627–3634.

Tzamarias,D. and Struhl,K. (1995) Distinct TPR motifs of CYC8 are involved in recruiting the CYC8–TUP1 corepressor complex of differentially regulated promoters. *Genes Dev.*, **9**, 821–831.

Xiao,B., Smerdon,S.J., Jones,D.H., Dodson,G.G., Soneji,Y., Altken,A. and Gamblin,S.J. (1995) Structure of a 14-3-3 protein and implications for coordination of multiple signalling pathways. *Nature*, **376**, 188–191.

Received November 21, 1997; revised January 7, 1998; accepted January 8, 1998